Electronic Supplementary Information

Ultrathin 2D Nickel Zeolitic Imidazolate Framework Nanosheets for Electrocatalytic Reduction of CO_2

Jian-Xiang Wu, Wei-Wen Yuan, Ming Xu, and Zhi-Yuan Gu*

Jiangsu Key Laboratory of Biofunctional Materials, Jiangsu Collaborative Innovation Center of Biomedical Functional Materials, Jiangsu Key Laboratory of New Power Batteries, School of Chemistry and Materials Science, Nanjing Normal University, Nanjing, 210023, P. R. China

Email: guzhiyuan@njnu.edu.cn, Fax/Phone: +86-25-85891952

Contents

Section S1. Experimental Section

Chemicals. The following chemicals were used as received without further purification: nickel acetate, imidazole, normal propyl alcohol, ammonium hydroxide, acetone, methyl alcohol, were purchased from Aladdin. Nafion D-521 dispersion (5 wt% in lower aliphatic alcohols and water) and Nafion 117 proton exchange membrane were purchased from Shanghai Hesen Electric Co. Ltd.. Toray carbon paper (TGP-H-60) was purchased from Alfa Aesar (China) Chemical Co. Ltd.. The ultrapure water (18.4 MΩ cm) was prepared by an ELGA purification system (Veolia Water Solutions & Technologies, UK).

Materials Characterization. X-ray diffraction (XRD) patterns were obtained from a Rigaku SmartLab 9 Kw instrument (Tokyo, Japan) D/MAX-2500 diffractometer with a Cu K_α radiation (1.54056 Å). Data was recorded from 5º to 50º. Transmission electron microscopy (TEM) images were recorded on a JEOL JEM-2100F transmission electron micro-scope operated at an accelerating voltage of 200 kV. Atomic force microscopy (AFM) measurements were per-formed with a PicoPlus in tapping mode (Agilent, US). X-ray photoelectron spectroscopy (XPS) were ESCALAB 250XI-AES (Thermo Fisher Scientific) equipped with Al Kα monochromator.

Preparation method of bulk $Ni(Im)_2$. Imidazole (1.17 g, 17 mmol) was added to a 50 mL of nickel (II) acetate (500 mg, 2.83 mmol) aqueous solution. Then, ammonium hydroxide (5 mL) was added to dark blue solution. A yellow precipitate appeared within 5 hours of heating to 100 ºC to obtain the polycrystalline material.

The yellow powder filtered and washed with water (4×30 mL) and acetone (2×30 mL) and dried in vacuum oven.[1]

Preparation method of 2D $Ni(Im)_2$-140 nm, 2D $Ni(Im)_2$-65 nm, 2D $Ni(Im)_2$-15 nm and 2D $Ni(Im)_2$-5 nm. In a typical process of liquid exfoliation, 80 mg of pristine bulk $Ni(Im)_2$ was ultrasonicated in 120 mL of a mixed solvent of methanol and n-propanol (1:1, v/v) for 4 h. After centrifugation at 500 rpm for 5 min, the collected supernatant was further centrifuged at 1000 rpm for 20 min. The precipitant of the 2D $Ni(Im)_2$-140 nm nanosheets was obtained and dried at room temperature overnight. Then the collected supernatant was further centrifuged at 3000 rpm for 20 min. The precipitant of the 2D $Ni(Im)_2$-65 nm nanosheets was obtained and dried at room temperature overnight. After that, the collected supernatant was further centrifuged at 10000 rpm for 20 min. The precipitant of the 2D $Ni(Im)_2$-15 nm nanosheets was obtained and dried at room temperature overnight. After that, the collected supernatant further centrifuged at 15000 rpm for 20 min. The precipitant of the 2D $Ni(Im)_2$-5 nm nanosheets was obtained and dried at room temperature overnight.[2]

Electrochemical Study. To prepare the electrode, catalyst (1 mg) prepared above were suspended in 50 μL ethanol with 10 μL Nafion D-521 dispersion (5 wt%) to form a homogeneous ink assisted by ultrasound. Then, 60 μL of the ink was spread onto the carbon paper (1×1 cm^2) surface by a micropipette and then dried under room temperature. The loading capacity of catalyst was 1 mg/cm^2. Before experiment, all the auxiliary electrodes were sonicated in HCl solution for 10 min and then washed

sequentially with water, acetone and ethanol. The electrochemical workstation (CHI 660E, Shanghai CH Instruments Co., China) was used in all the experiments of CO_2 reduction. Cyclic voltammetry (CV) and linear sweep voltammetry (LSV) measurements were carried out in a typical H-Type cell with three-electrode configuration, which consisted of working electrode, a platinum sheet auxiliary electrode, and a Ag/AgCl reference electrode. The electrolyte was bubbled with N_2 or CO_2 for at least 30 min to form N_2 or CO_2 saturated solution. The LSV measurement in gas-saturated electrolyte was conducted in the potential range of 0 to -1.2 V vs. RHE at a sweep rate of 50 mV/s in N_2-saturated 0.5 M $KHCO_3$ (pH=8.4) and CO_2-saturated 0.5 M $KHCO_3$ (pH=7.2) as supporting electrolyte. The potentials in the study were reported versus RHE with the conversion E (vs. RHE) = E (vs. Ag/AgCl) + 0.21 V + 0.059 × pH. The electrolysis experiments were conducted at 25 ^oC in a typical H-type cell. In the experiments, the cathode and anode compartments were separated through a Nafion 117 proton exchange membrane. Hydrion can be transferred from anode compartment to cathode compartment through Nafion 117 proton exchange membrane. Potassium bicarbonate (0.5 M) aqueous solution was employed as an electrolyte at ambient temperature.

Section S2. Data Processing Section

Product analysis. The gaseous product of electrochemical experiments was analyzed online by gas chromatography (GC, SRI, 8610C), which was equipped with helium ionization detector (HID) and thermal conductivity detector (TCD) using helium (99.999%) as the carrier gas. The online gas analysis was performed with the injection of 1 mL every time. The column effluent (separated gas mixtures) was first passed through a TCD and then passed through a HID. Their faradic efficiency was calculated as follows:

$$FE(\%) = \frac{J_{CO}}{J_{total}} = \frac{v_{co} \times z \times F}{J_{total}} \times 100\%$$

J_{CO} : partial current density for CO production;

J_{total}: total current density;

z: the number of electron transferred for product formation, which is 2 for CO;

v_{CO}: the production rate of CO (measured by GC);

F: Faradaic constant, 96485 C/mol;

FE: faradaic efficiency for CO production.

Calculation of surface active sites. We integrated the anodic wave in the CV curve of $Ni(Im)_2$ under N_2, and then calculated the amount of quantity of electric charge: [3]

$$Q = \frac{S}{v}$$

Q: the integrated charge of the anodic wave;

S: the oxidation peak area of the cyclic voltammetry curve and v is the sweep speed.

The amount of surface active Ni(II) sites by assuming a one-electron redox process:

$$n = \frac{Q}{F}$$

n: the amount of surface active Ni on the working electrode;

Q: the integrated charge of the anodic wave;

F: Faraday constant, 96485 C mol^{-1}.

Calculation of Turnover Frequency (TOF, h^{-1}). The TOF for CO was calculated as:

$$TOF = \frac{(J_{product} / zF) / n_{tot}}{f} \times 3600$$

$J_{product}$: partial current for CO;

z: the number of electron transferred for product formation, which is 2 for CO;

F: Faradaic constant, 96485 C mol^{-1};

n_{tot}: the molar amount of Ni on the working electrode;

f: the surface fraction of electrochemically active Ni sites.

The total amount of Ni was calculated as follows:

$$n_{tot} = \frac{m_{cat} W_{Ni}}{M_{Ni}}$$

n_{tot}: the molar amount of Ni on the working electrode;

m_{cat}: the mass of the electrocatalyst loaded on the working electrode;

W_{Ni}: the weight fraction of Ni in the electrocatalyst determined;

M_{Ni}: the atomic weight of Ni.

Then, the surface fraction of electrochemically active Ni sites was determined as follows:

$$f = \frac{n}{n_{tot}}$$

Section S3. Supplementary Figures and Tables

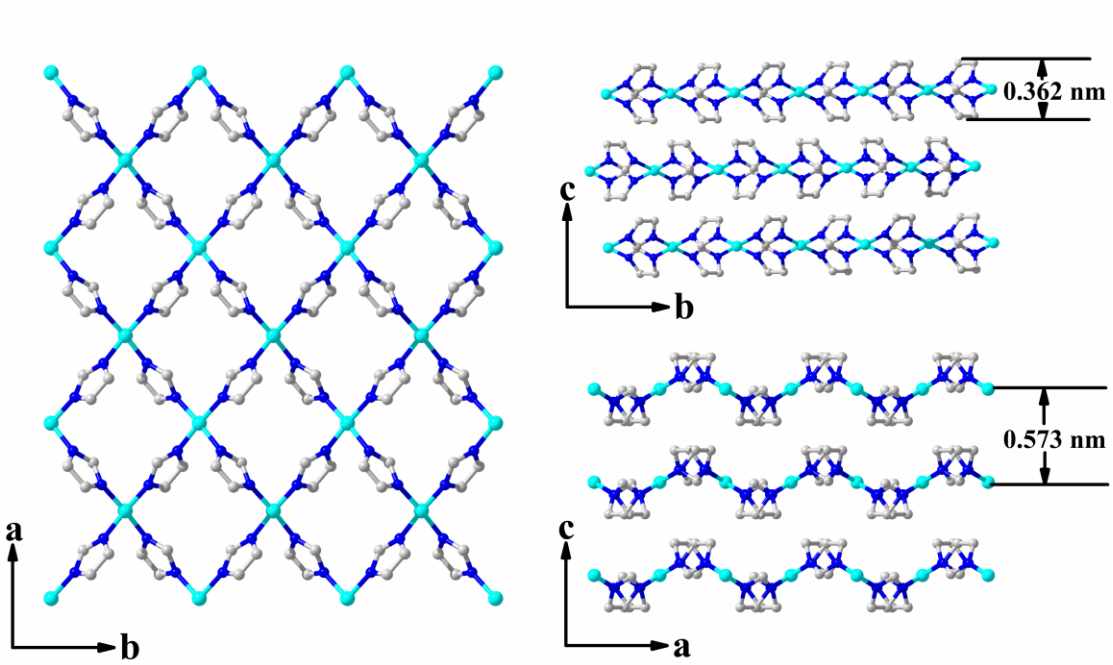

Fig. S1. Simulated crystal structures of $Ni(Im)_2$ under different view directions. Blue is N, grey is C and cyan is Ni.

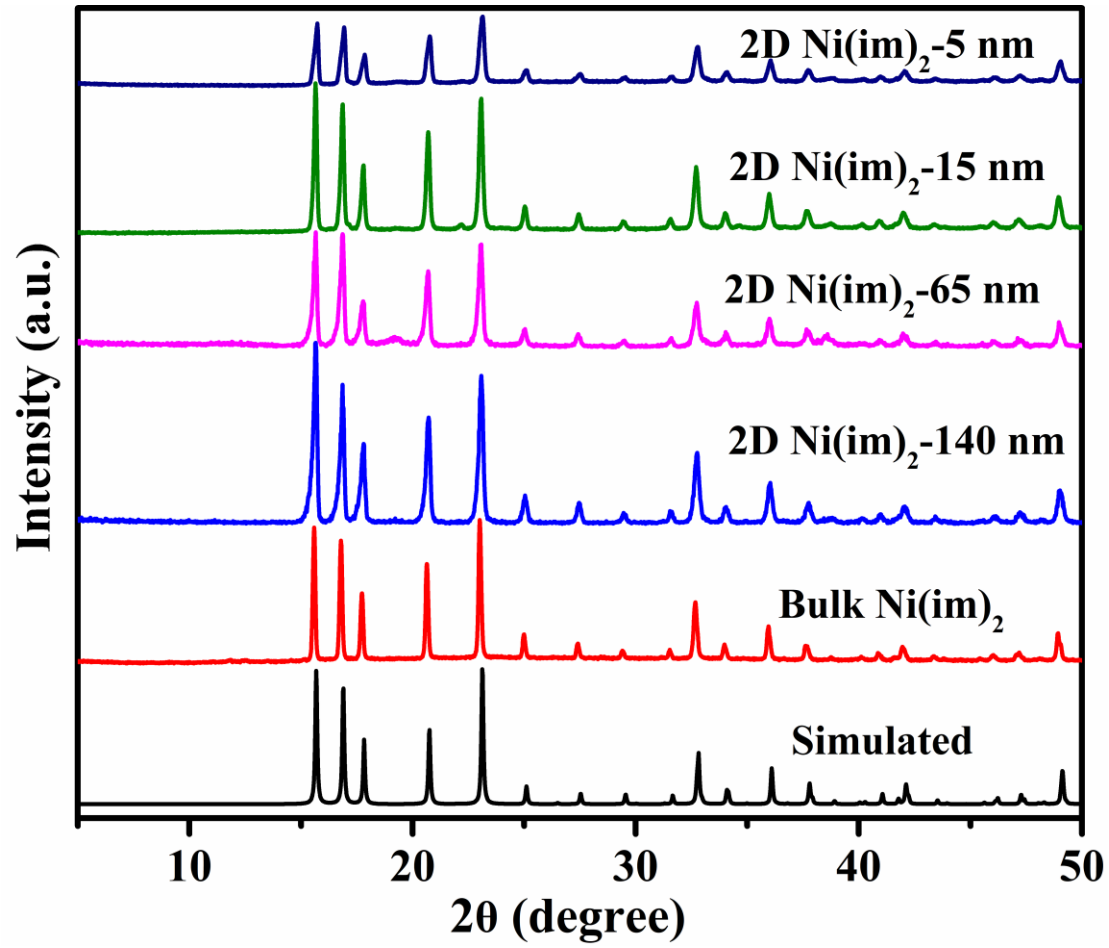

Fig. S2. Powder XRD patterns of bulk $Ni(Im)_2$ and 2D $Ni(Im)_2$ nanosheets with different thickness.

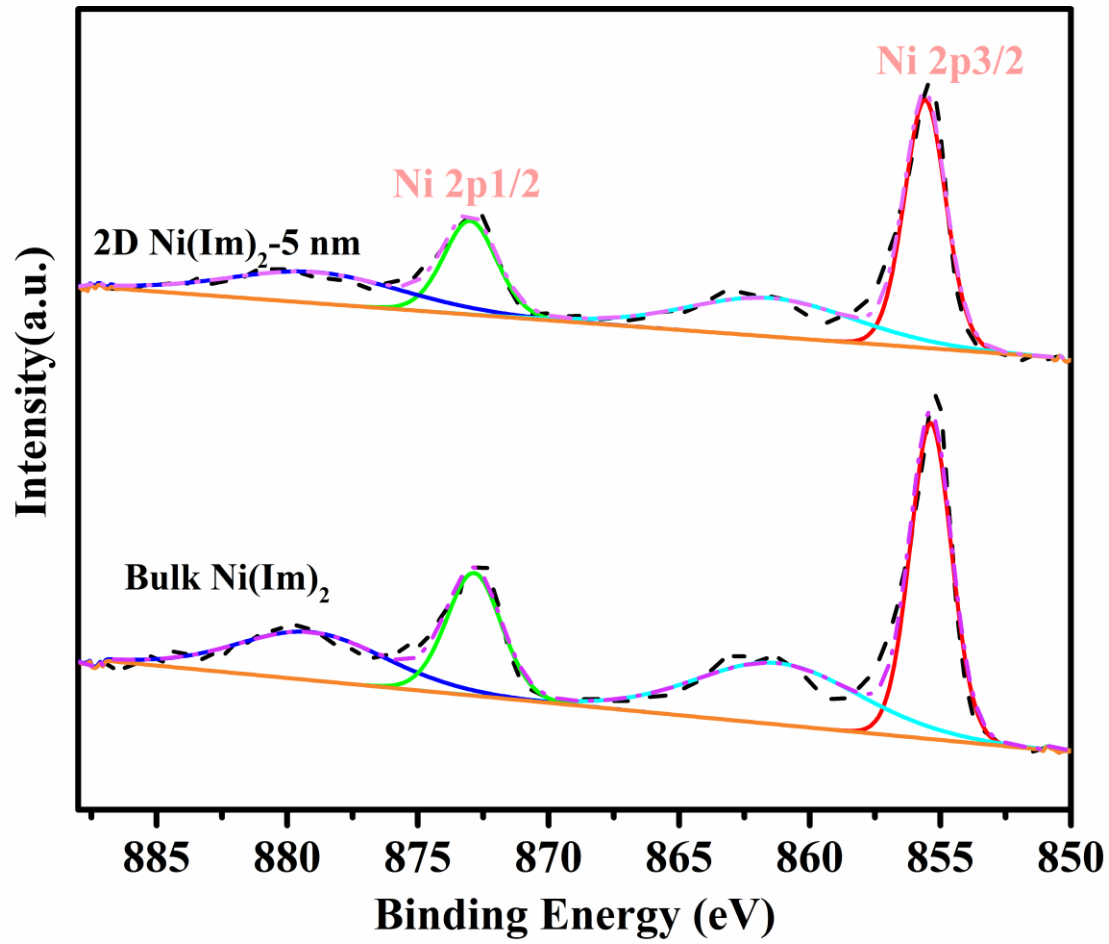

Fig. S3. XPS spectra of bulk $Ni(Im)_2$ and 2D $Ni(Im)_2$-5 nm nanosheets.

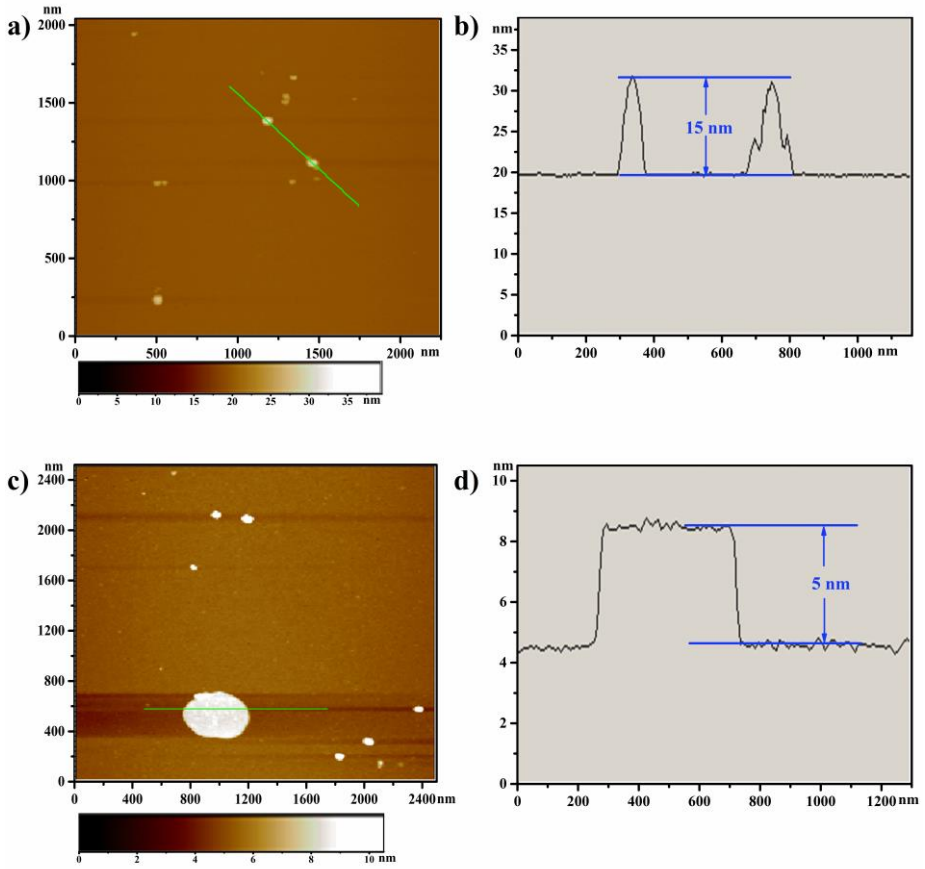

Fig. S4. (a) AFM image of 2D $Ni(Im)_2$-15 nm. (b) the thickness curve of 2D $Ni(Im)_2$-15 nm. (c) AFM image of 2D $Ni(Im)_2$-5 nm. (d) the thickness curve of 2D $Ni(Im)_2$-5 nm.

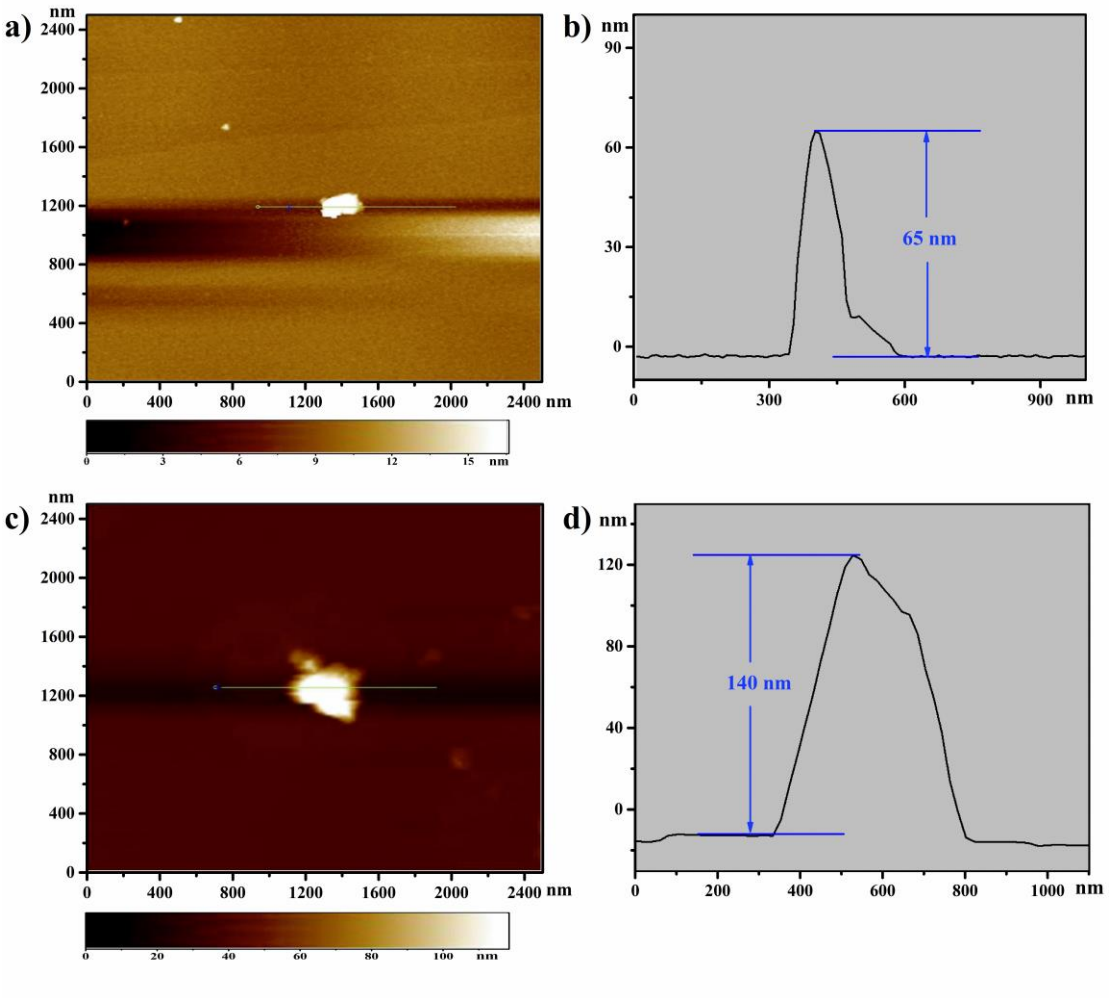

Fig. S5. (a) AFM image of 2D $Ni(Im)_2$-65 nm. (b) the thickness curve of 2D $Ni(Im)_2$-65 nm. (c) AFM image of 2D $Ni(Im)_2$-140 nm. (d) the thickness curve of 2D $Ni(Im)_2$-140 nm.

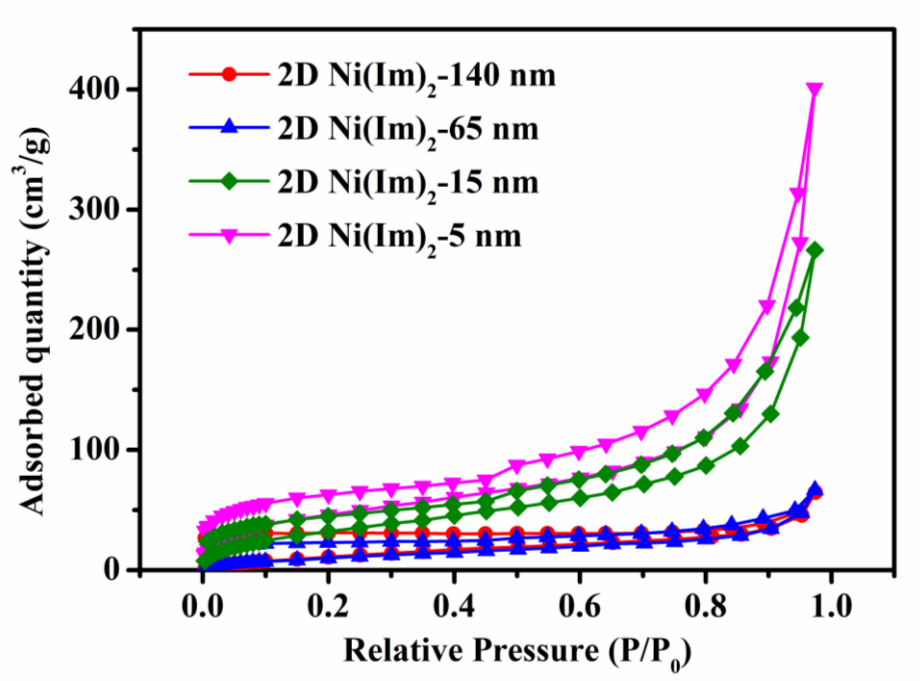

Fig. S6. N_2 adsorption-desorption isotherms of 2D $Ni(Im)_2$-140 nm, 2D $Ni(Im)_2$-65 nm, 2D $Ni(Im)_2$-15 nm and 2D $Ni(Im)_2$-5 nm.

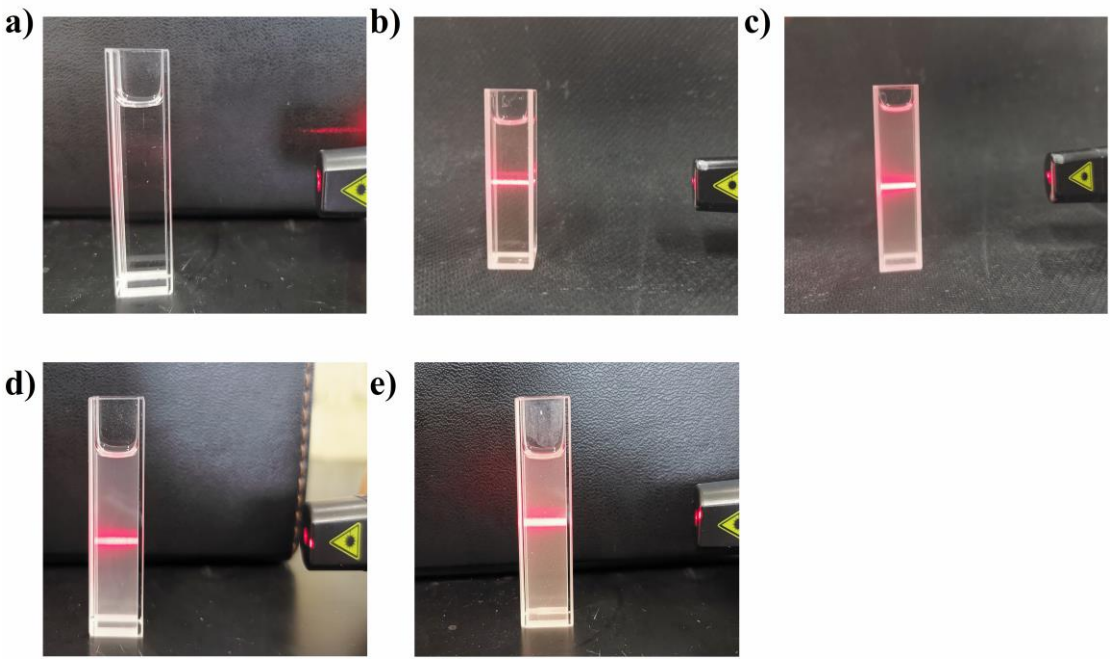

Fig. S7. (a) Photograph of bulk $Ni(Im)_2$ aqueous suspension. (b) Photograph of 2D $Ni(Im)_2$-140 nm suspension. (c) Photograph of 2D $Ni(Im)_2$-65 nm suspension. (d) Photograph of 2D $Ni(Im)_2$-15 nm suspension. (e) Photograph of 2D $Ni(Im)_2$-5 nm suspension.

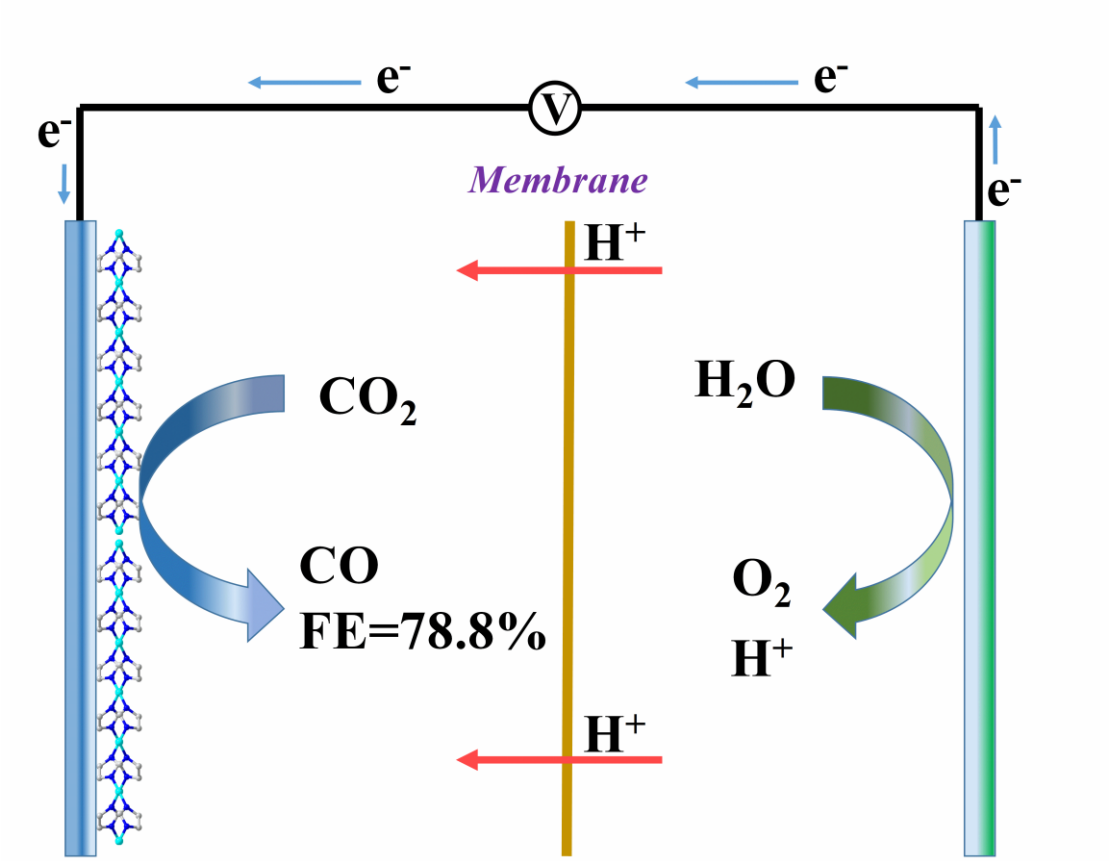

Fig. S8. CO_2 electrochemical reduction system with 2D $Ni(Im)_2$-5 nm nanosheets as the catalyst. $CO_2 + 2H^+ + 2e^- \rightarrow CO + H_2O$.

FE=(J_{co}/J_{total}) ×100% = (2×96485C/mol×2.043×10^{-8} mol/s)/(5 mA×10^{-3}) = 78.8%

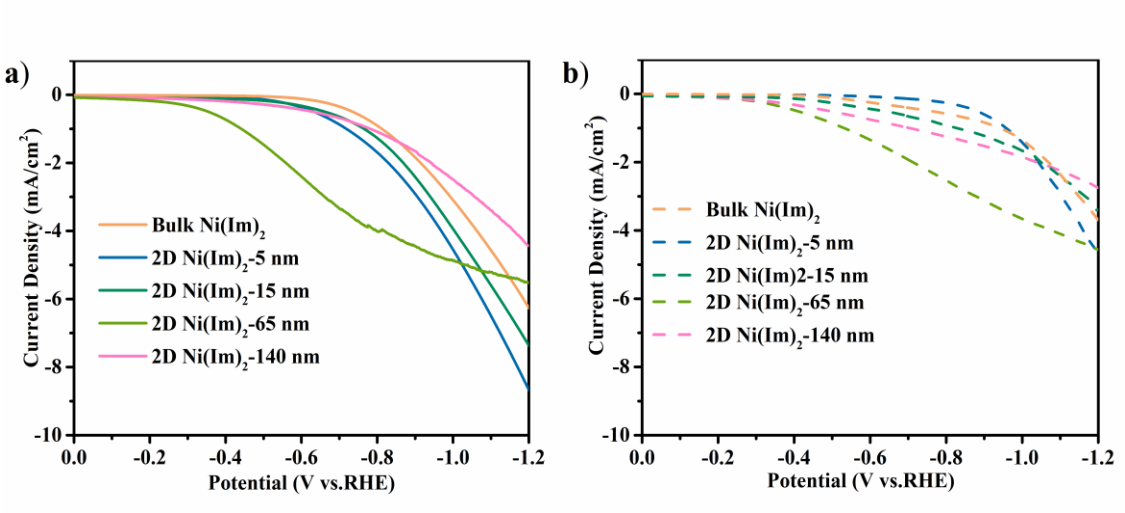

Fig. S9. (a) Linear sweep voltammetry of bulk $Ni(Im)_2$, 2D $Ni(Im)_2$-140 nm, 2D $Ni(Im)_2$-65 nm, 2D $Ni(Im)_2$-15 nm and 2D $Ni(Im)_2$-5 nm in CO_2-saturated 0.5 M $KHCO_3$. (b) Linear sweep voltammetry of bulk $Ni(Im)_2$, 2D $Ni(Im)_2$-140 nm, 2D $Ni(Im)_2$-65 nm, 2D $Ni(Im)_2$-15 nm and 2D $Ni(Im)_2$-5 nm in N_2-saturated 0.5 M $KHCO_3$.

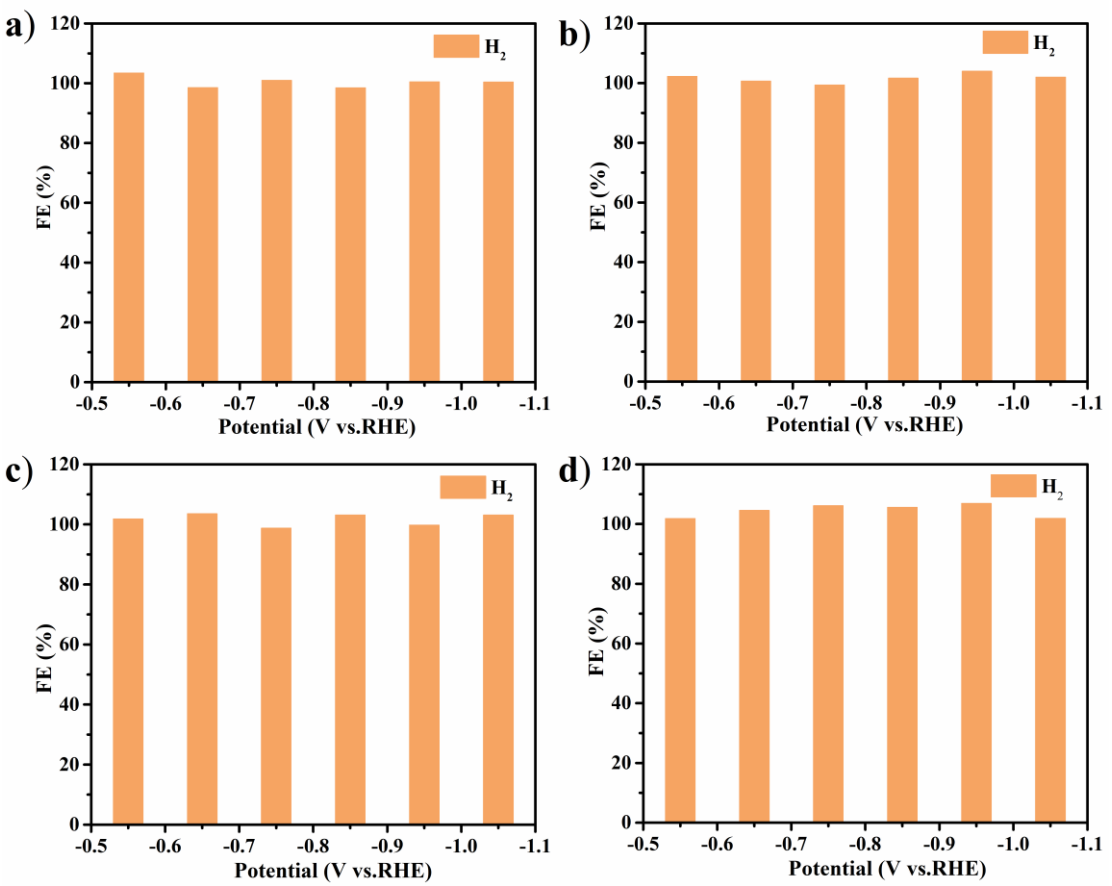

Fig. S10. Eletrocatalytic performance in N_2-saturated 0.5 M $KHCO_3$ for (a) 2D $Ni(Im)_2$-140 nm. (a) 2D $Ni(Im)_2$-65 nm. (a) 2D $Ni(Im)_2$-15 nm and (b) 2D $Ni(Im)_2$-5 nm measured by online GC.

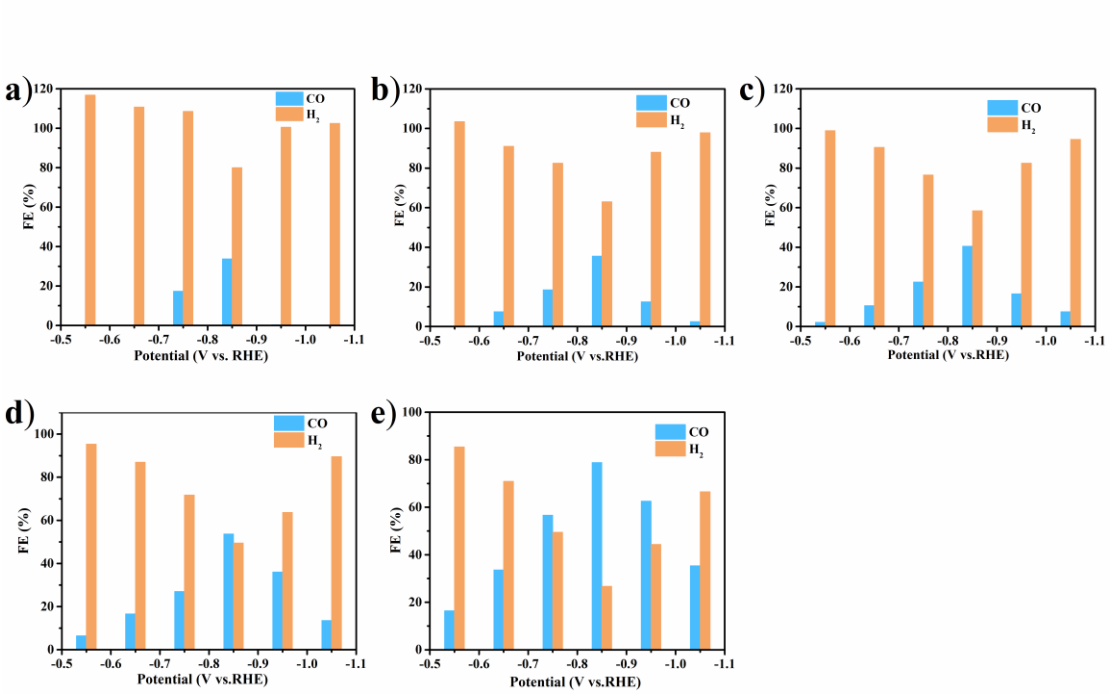

Fig. S11. CO_2RR performance in CO_2-saturated 0.5 M $KHCO_3$ using (a) bulk $Ni(Im)_2$. (b) 2D $Ni(Im)_2$-140 nm. (c) 2D $Ni(Im)_2$-65 nm. (d) 2D $Ni(Im)_2$-15 nm and (e) 2D $Ni(Im)_2$-5 nm as catalysts.

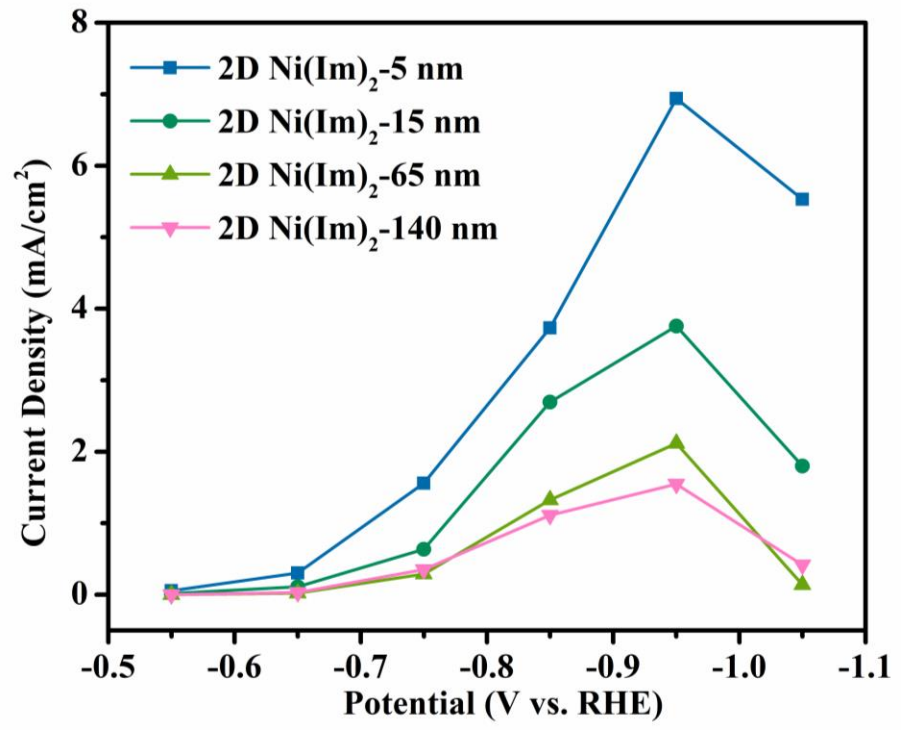

Fig. S12. Potential-dependent CO partial current densities on 2D $Ni(Im)_2$-140 nm, 2D $Ni(Im)_2$-65 nm, 2D $Ni(Im)_2$-15 nm and 2D $Ni(Im)_2$-5 nm.

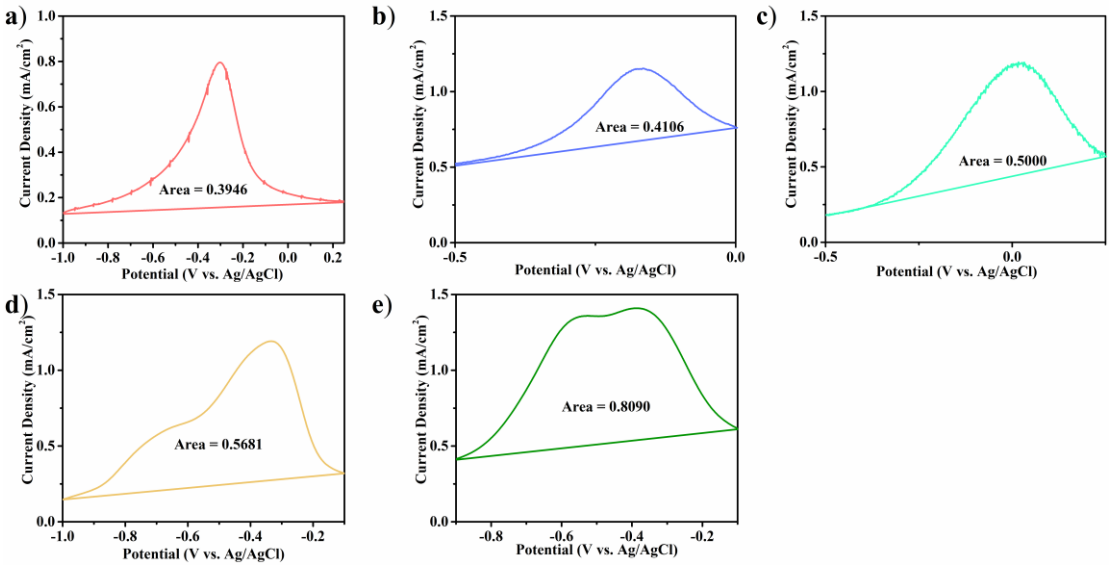

Fig. S13. Total charge integrated from anodic wave. With CV scan speed of 50 mV/s in N_2-saturated 0.5 M $KHCO_3$, we further estimated surface Ni active sites. (a) bulk $Ni(Im)_2$. The amount of surface active n_{Ni} = [0.3946 (mA·V/cm^2) / 50 (mV/s)] / 96485 C/mol = 8.17×10^{-8} mol/cm^2. (b) 2D $Ni(Im)_2$-140 nm. The amount of surface active n_{Ni}= [0.4106 (mA·V/cm^2) / 50 (mV/s)] / 96485 C/mol = 8.51×10^{-8} mol/cm^2. (c) 2D $Ni(Im)_2$-65 nm. The amount of surface active n_{Ni}= [0.5000 (mA·V/cm^2) / 50 (mV/s)] / 96485 C/mol = 1.04×10^{-7} mol/cm^2. (d) 2D $Ni(Im)_2$-15 nm. The amount of surface active n_{Ni}= [0.5681 (mA·V/cm^2) / 50 (mV/s)] / 96485 C/mol = 1.18×10^{-7} mol/cm^2. (e) 2D $Ni(Im)_2$-5 nm. The amount of surface active n_{Ni}= [0.8090 (mA·V/cm^2) / 50 (mV/s)] / 96485 C/mol = 1.68×10^{-7} mol/cm^2. The broad peaks may be resulted from the multiple redox processes.

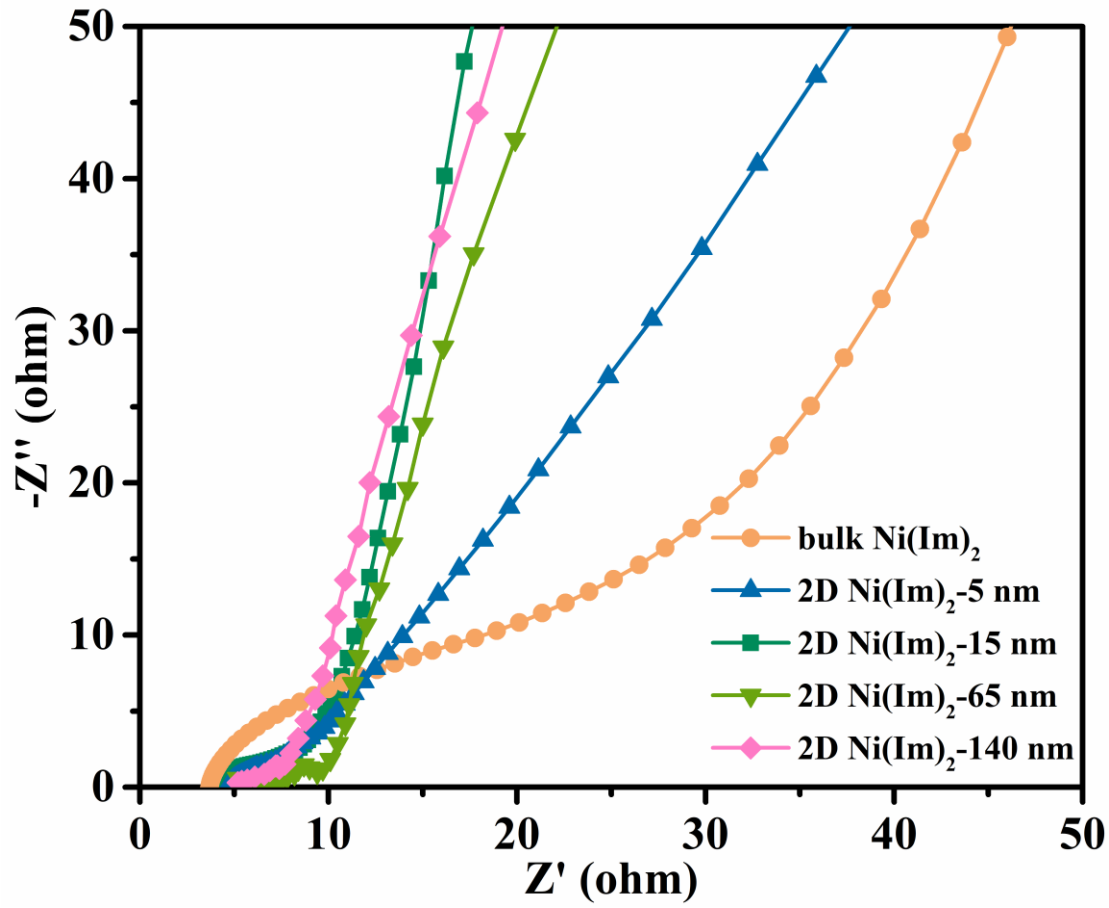

Fig. S14. Electrochemical impedance spectroscopy (EIS) for bulk $Ni(Im)_2$, 2D $Ni(Im)_2$-140 nm, 2D $Ni(Im)_2$-65 nm, 2D $Ni(Im)_2$-15 nm and 2D $Ni(Im)_2$-5 nm. EIS measurements were done with a frequency range from 100 kHz to 0.01 Hz at a 5 mV amplitude referring to open circuit potential.

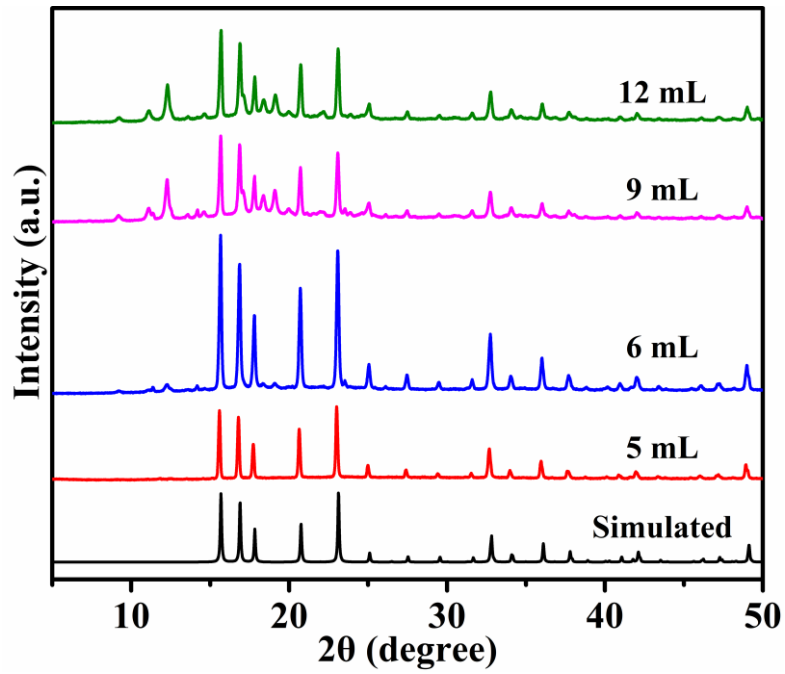

Fig. S15. Powder XRD patterns of Ni-MOF with different amount of ammonium hydroxide in the process of synthesis.

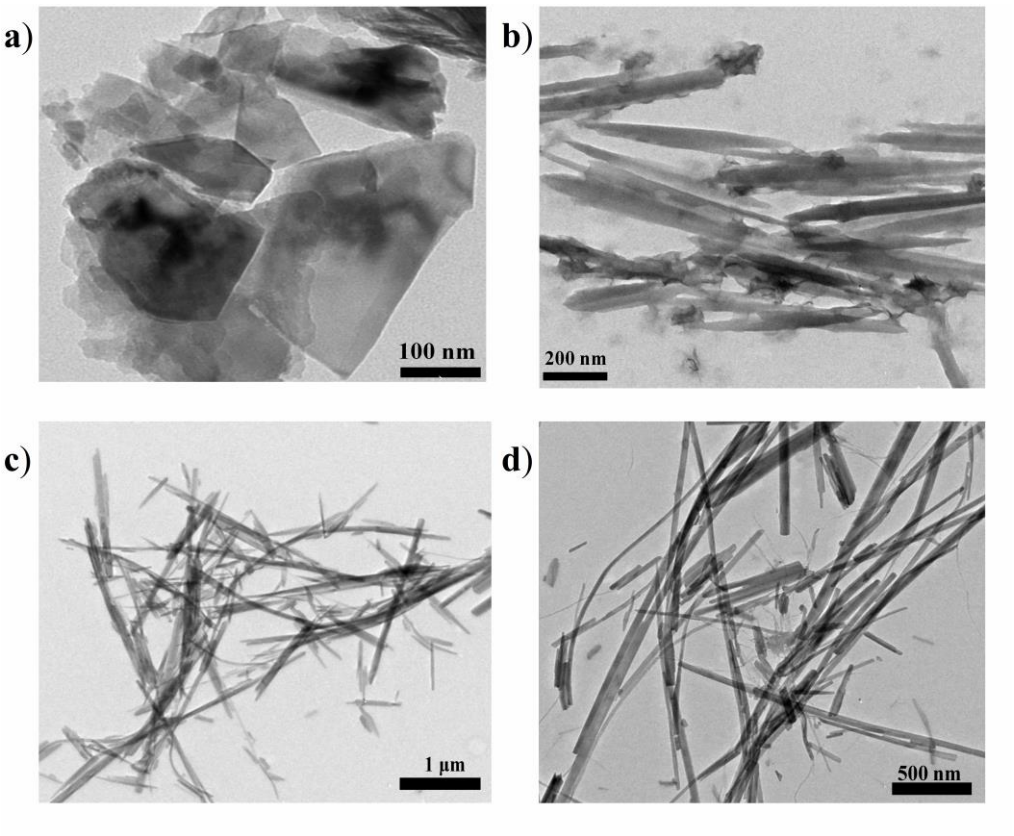

Fig. S16. TEM of Ni-MOF with different amount of ammonium hydroxide in the process of synthesis after exfoliation. (a) 5 mL. (b) 6 mL. (c) 9 mL. (d) 12 mL.

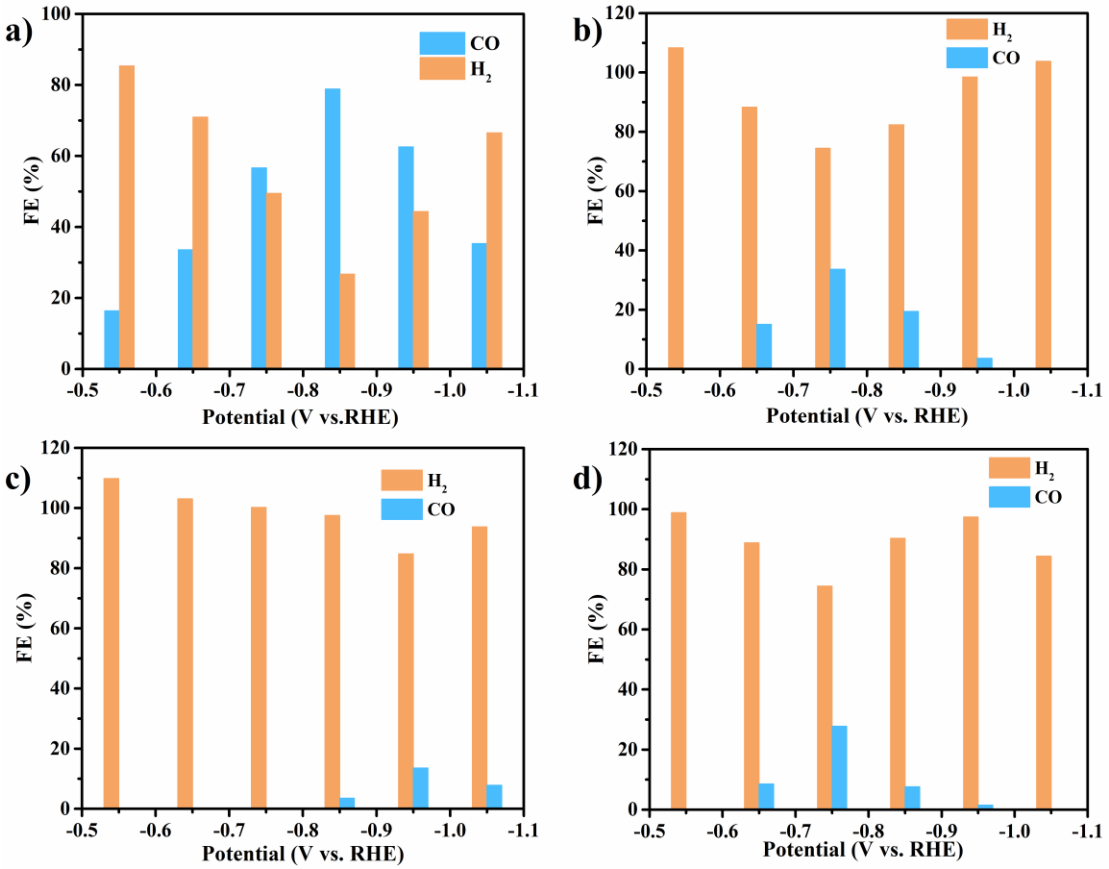

Fig. S17. FEs of Ni-MOF with different amount of ammonium hydroxide in the process of synthesis. (a) 5 mL. (b) 6 mL. (c) 9 mL. (d) 12 mL.

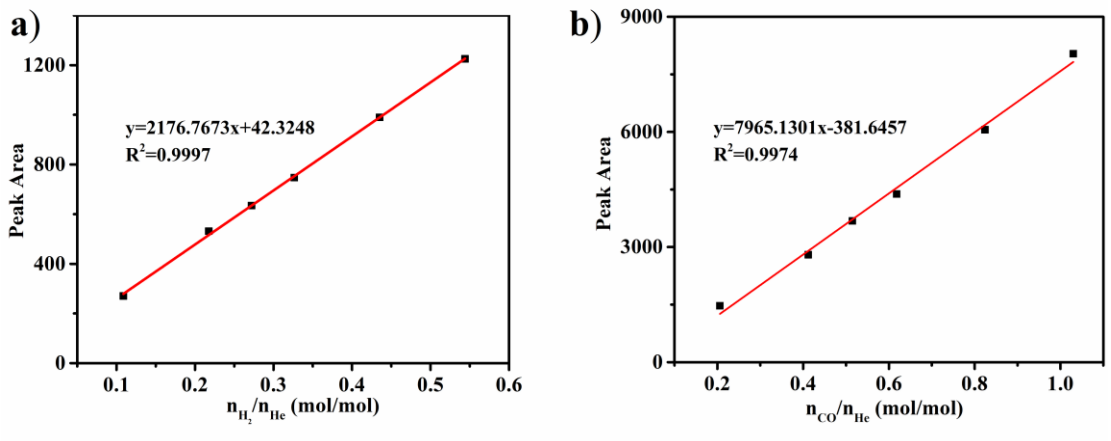

Fig. S18. Standard curves for (a) H_2 and (b) CO in GC measurements.

Section S4. References

1. N. Masciocchi, F. Castelli, P. M. Forster, M. M. Tafoya and A. K. Cheetham, *Inorg. Chem.*, 2003, **42**, 6147-6152.
2. H.-L. Liu, Y.-J. Chang, T. Fan and Z.-Y. Gu, *Chem. Commun.*, 2016, **52**, 12984-12987.
3. (a) N. Han, Y. Wang, L. Ma, J. Wen, J. Li, H. Zheng, K. Nie, X. Wang, F. Zhao and Y. Li, *Chem*, 2017, **3**, 652-664; (b) N. Han, Y. Wang, H. Yang, J. Deng, J. Wu, Y. Li and Y. Li, *Nat. Commun.*, 2018, **9**, 1320.